

Control of microstructure and disintegration properties of silica granules from PVA slurries by spray drying

TOSHIHIRO ISHIMORI

Division of Research & Development, KOSE Corporation, Kita-ku, Tokyo 114, Japan

MAMORU SENNA

Faculty of Science and Technology, Keio University, Hiyoshi, Yokohama 223, Japan

The microstructure of spray-dried model granules, comprising silica microspheres and poly(vinylalcohol), was observed by scanning electron microscopy (SEM) and transmission electron microscopy (TEM) with an ultramicrotome technique. Disintegration of granules was characterized by a shear method for granular beds, and by a compression test for single granules. The internal structure changed significantly with the pH of the slurry from which the granules were spray-dried. Granules from pH 7 slurry showed the smallest apparent density, and were disintegrated under the smallest applied load. By analysing the relationship between microstructure, apparent density and flow behaviour of the slurries, it was possible to obtain a guideline for preparation of appropriate granules with controlled microstructure and strength.

1. Introduction

Granulation of powders are carried out for various purposes, e.g. to improve handling or packing, for the utility of catalysts, to obtain better feeling, and have a new function in cosmetics for make-up [1]. It is particularly important to measure and control disintegration behaviour so that the appropriate choice of granule can be made.

Hitherto, correlation between the microstructure and strength of a spray-dried granule, comprising a silica microsphere and poly(vinylalcohol) (PVA), has been studied [2]. The role of PVA as a binder has been thoroughly studied from a practical point of view, e.g. to obtain homogeneous green bodies and to improve mechanical properties in the field of ceramic fabrication [3–5]. For the purpose of controlling granule microstructure, however, further studies are still necessary to understand fully the role of PVA in a slurry compared to that in spray-dried granules, i.e. in the processes of flowing, atomizing and drying.

PVA is used as an additive for the control of slurry viscosity. In colloid chemistry, the role of PVA has mainly been observed from adsorption behaviour to the particles [6–9]. PVA adsorption takes place by hydrogen bonding between hydroxyl groups of PVA and the silica surface. The difference between the interior and surface structure of granules comprising the different additives, has been preliminarily studied [2]. By comparing granules containing Aerosil and silica sol as additives, it was found that the difference between the interior and surface structure of the granule was greater for those containing Aerosil. This

difference can be attributed to the dispersion state of particles in the slurry.

The purpose of the present study is to elucidate development of the microstructure and strength of granules, by varying slurry conditions under controlled pH, in an attempt to obtain a guideline for designing a granule with controlled microstructure and strength.

2. Experimental procedure

2.1. Materials

Granules were prepared by a spray drying method. Details are described elsewhere [10]. The composition of each granule is given in Table I. Granules obtained from slurries comprising only silica microspheres and poly(vinylalcohol) are categorized as group A, while those containing ultra-fine powder (Degussa, Aerosil 200^R, $d_{50} = 12$ nm) are categorized as group B. Slurries of silica microspheres (Suzuki Yushi, God ball^R, median diameter, $d_{50} = 1.5$ μ m) were prepared using a 20 wt% aqueous solution of poly(vinylalcohol) (Kuraray, Poval 217^R, polymerization degree, 1750, saponification value, 87%). The pH of these slurries was adjusted to 3, 5, 7, 9 and 11 with 1 N NaOH or 1 N HCl.

2.2. Characterization

A commercial coaxial cylindrical rheometer (Contravs, Rheomat 115) was used to measure the flow properties of the slurry at 20 ± 1 °C. The steady state

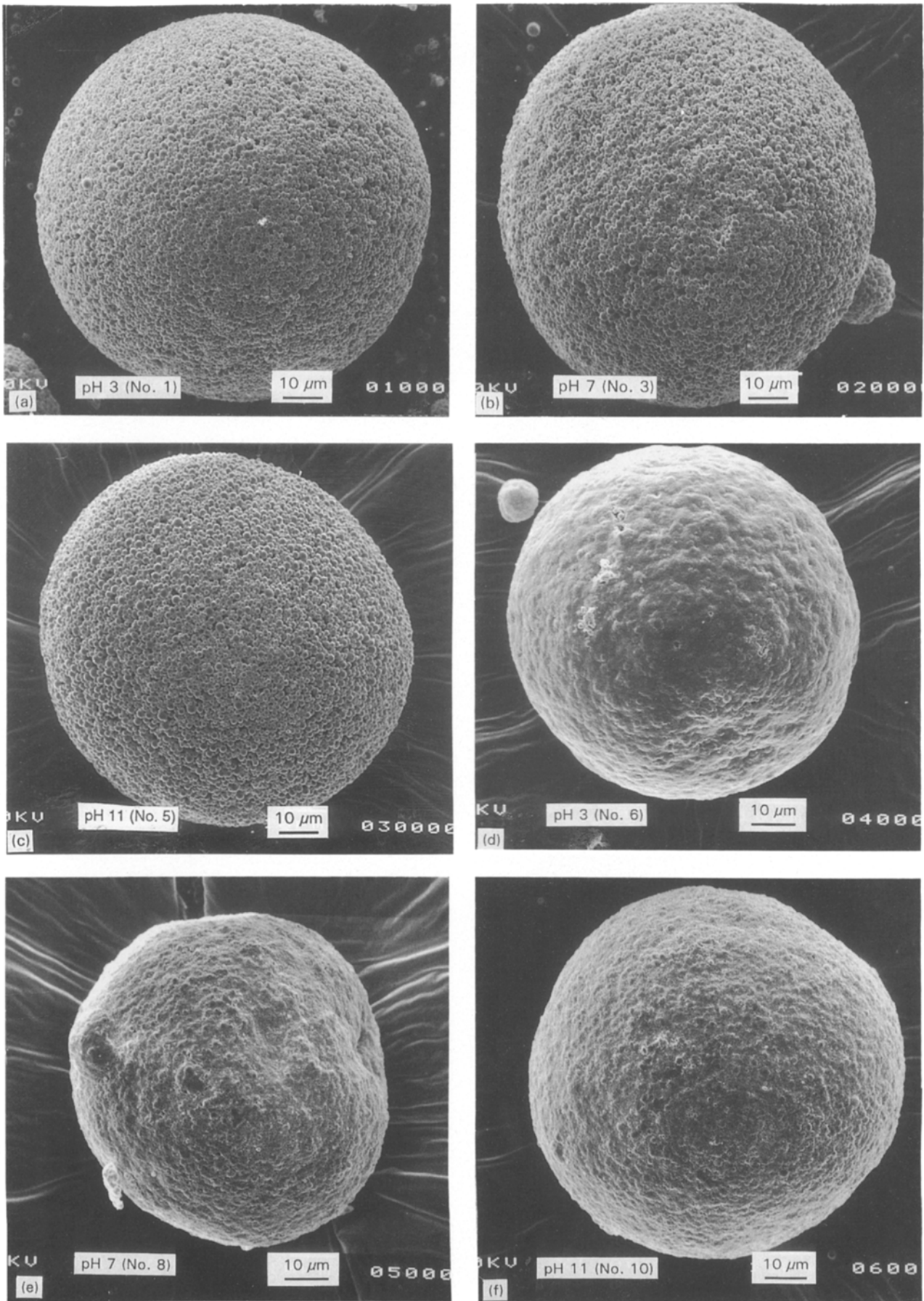


Figure 1 Representative scanning electron micrographs of granules.

rheological properties were analysed under a Bingham approximation to obtain the plastic viscosity, η_{pl} , and Bingham yield value, t_B . The effective volume fraction of flocs, Φ_F , and the bulkiness, C_{FP} , the latter being the ratio of Φ_F to the solid fraction, Φ_p , were determined. C_{FP} was calculated from η_{pl} by the Thomas equation [11]. The dehydration process was analysed by thermogravimetry at 70 °C.

The surface structure was observed under a scanning electron microscope (SEM), while the interior of the granule was observed by a transmission electron microscope (TEM). Samples used for TEM observation were prepared by embedding the granules in an epoxy resin, and were cut in thin slices by an ultra-

microtome. The apparent density of granules was determined from pore size distribution by a mercury porosimeter (Caluro Elba 220).

For the purpose of compressive shear testing of the granular bed, a commercial surface tester (Heidon 14) was used, as described previously [10]. The resistance index, μ , was defined as the measured resistance divided by the compressive stress. When the compressive stress exceeded a critical value, the shear resistance began to increase showing the yield point of the granular layer. The range of the compressive stress at which the granular bed collapsed, henceforth called the compressive shear strength, β , was determined from the analogue output profile of the surface tester.

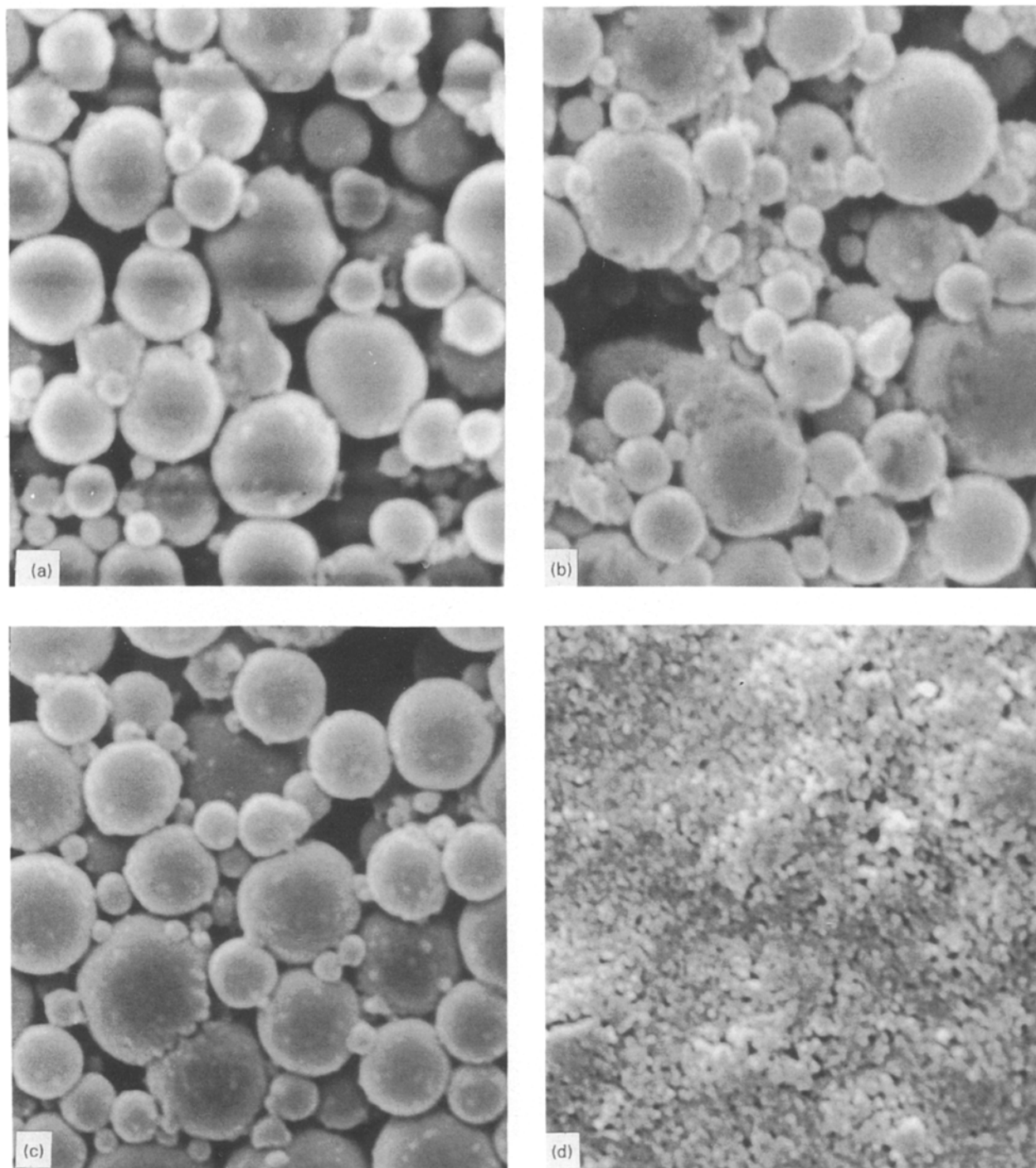


Figure 2 Scanning electron micrographs of granule surfaces at higher magnification. (a) pH 3 (No. 1), (b) pH 7 (No. 3), (c) pH 11 (No. 5), (d) pH 3 (No. 6), (e) pH 7 (No. 8) and (f) pH 11 (No. 10).

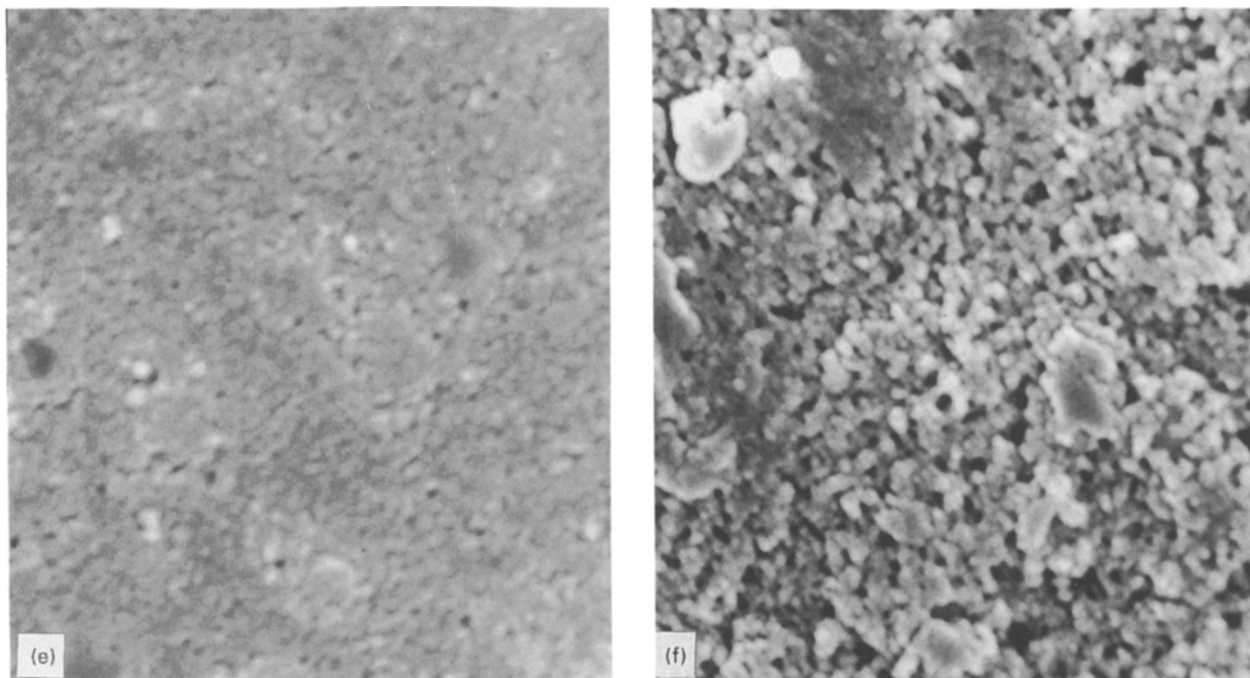


Figure 2 (continued)

TABLE I Composition and properties of slurry and granules

Group Sample No.	A					B				
	1	2	3	4	5	6	7	8	9	10
Composition ^a (%)										
Silica beads ^b	90	90	90	90	90	70	70	70	70	70
Fumed silica ^c	—	—	—	—	—	20	20	20	20	20
Polyvinylalcohol ^d	10	10	10	10	10	10	10	10	10	10
Slurry										
Φ_D^e	0.10	0.10	0.10	0.10	0.10	0.11	0.11	0.11	0.11	0.11
pH	3.04	5.04	6.88	9.96	10.9	2.97	5.01	6.97	8.40	10.9
Plastic viscosity, η_{DI} (MPaS)	12	8	55	42	14	179	213	301	254	27
Bingham yield value, τ_B (Pa)	0.05	0.70	2.05	0.80	0.05	22.4	21.3	18.6	7.20	0.49
C_{FF}^f	1.19	1.44	4.05	3.59	1.78	4.98	5.00	5.22	5.11	3.82
Granule										
Total pore volume ($10^{-3} \text{ m}^3 \text{ kg}^{-1}$)	1.05	1.08	1.11	1.02	0.76	0.93	0.96	0.97	0.86	0.71
Particle density (10^3 kg m^{-3})	0.95	0.93	0.90	0.98	1.32	1.08	1.04	1.03	1.16	1.41
Pore size (nm)	208	174	194	179	190	42	56	64	39	33
β^f (kPa)	3.5–4.0	2.0–2.5	2.0–2.5	3.5–4.0	4.5–5.0	5.5–6.0	4.5–5.0	4.0–4.5	5.5–6.0	10.5–11.0

^aAll samples contain 20 parts by weight of ethylalcohol and 280 parts by weight of 0.01 M NH_4Cl aq.

^b God-ball® (Suzuki-yushi, median diameter, $d_{50} = 1.5 \mu\text{m}$) ^c Aerosil® 200 (Degussa)

^dPoval 217c® (Kuraray, polymerization degree 1750, saponification value, 87%)

^eVolume % of powder

^fCompressive-shear strength of granule bed

3. Results and discussion

3.1. Microstructure of granules

3.1.1. Surface structure

The surface structure of group A and B granules is shown in Figs 1 and 2, respectively. From the micrographs, it is recognized that the surface of group A

granules consisted of a network of host microspheres, showing no significant difference due to the change in slurry composition. The surface of group B granules was much smoother and varied with the pH of the starting slurry. The pores at the surface were stuffed with microparticles (Aerosil).

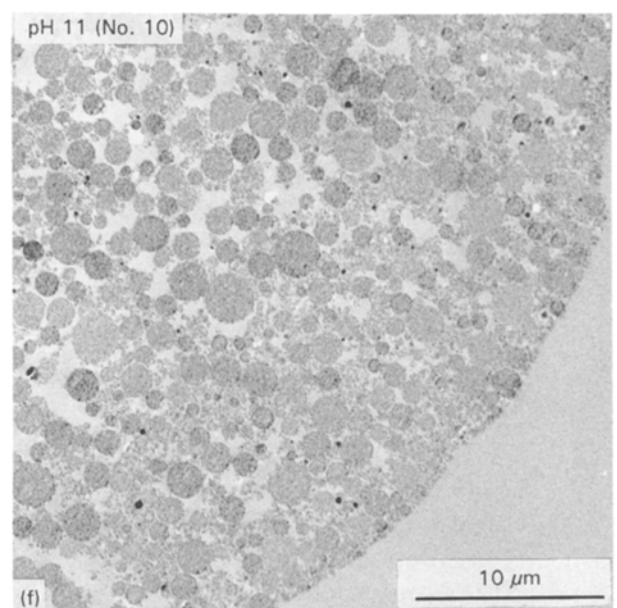
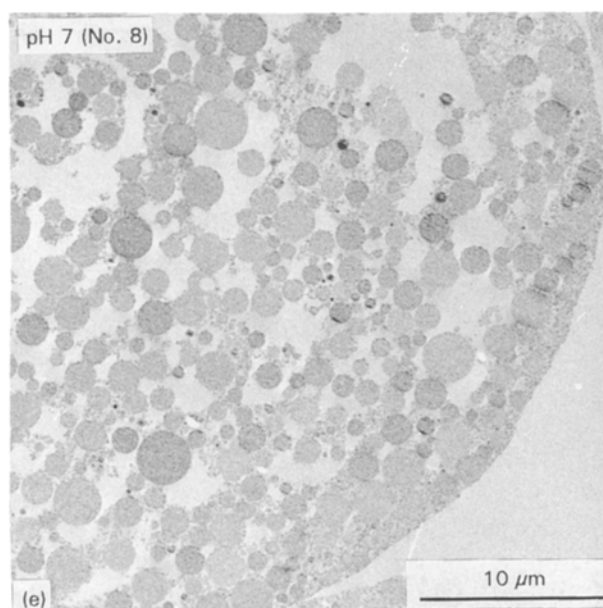
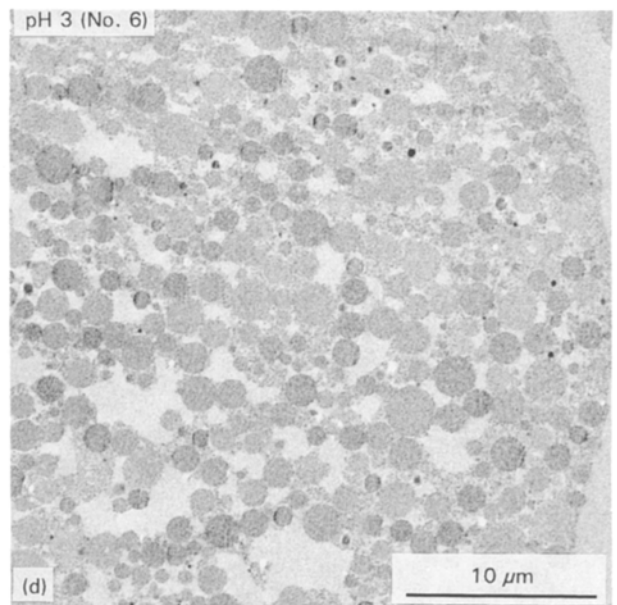
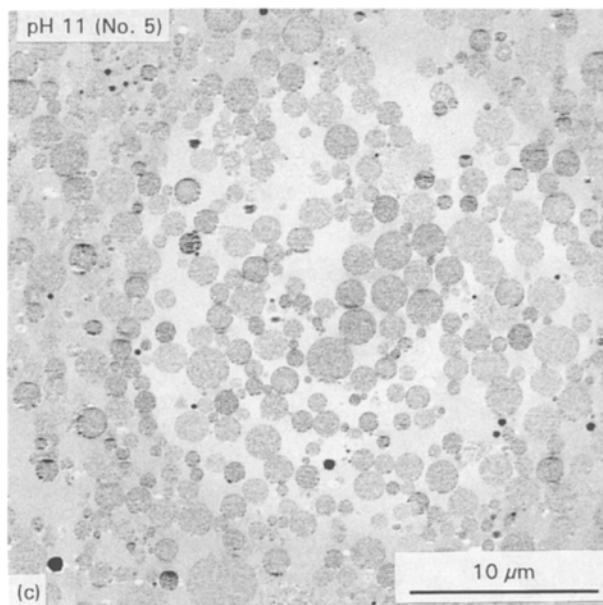
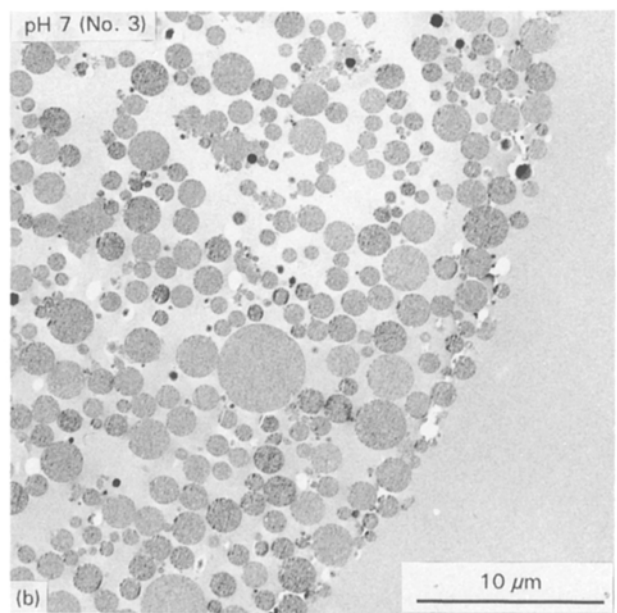
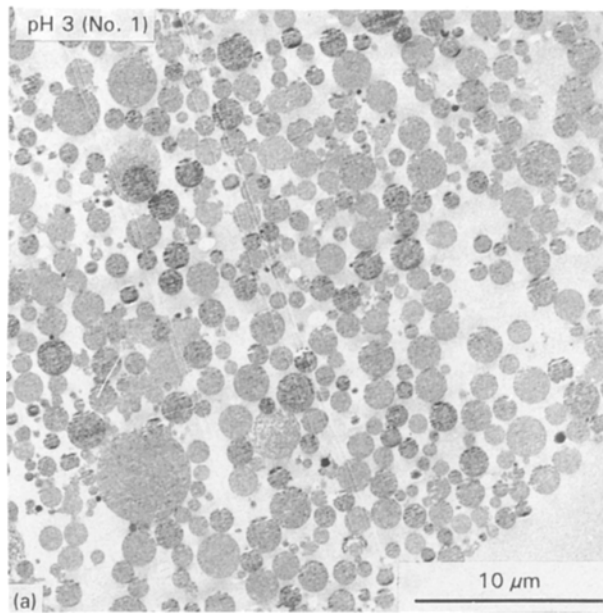


Figure 3 Representative transmission electron micrographs of sliced section of granules embedded in epoxy resin.

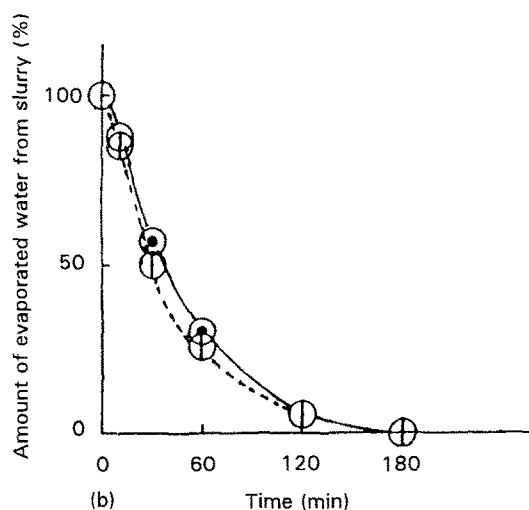
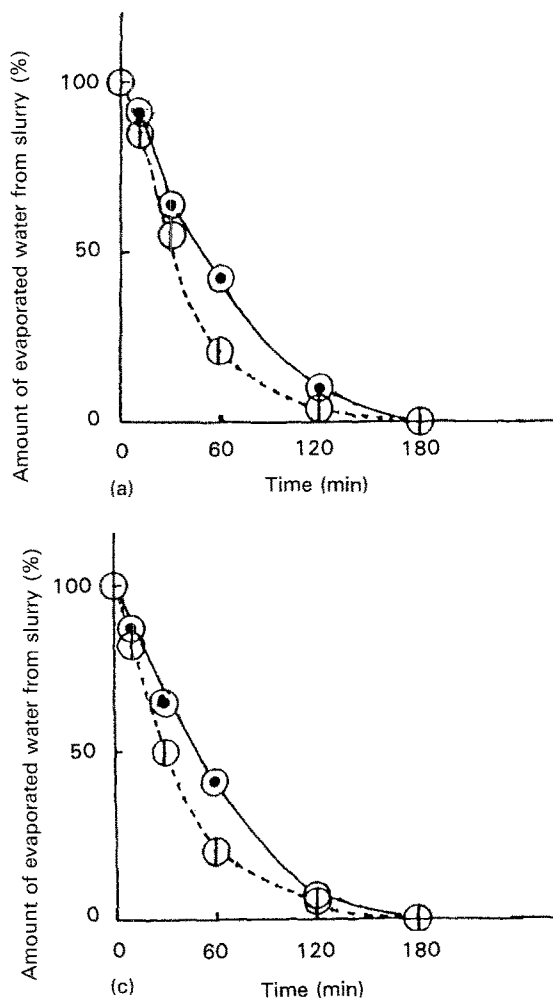


Figure 4 Isothermal dehydration curves of slurries at 70 °C (a) pH 3, (b) pH 7 and (c) pH 11. (○) A group; (●) B group.

3.1.2. Internal structure

Fig. 3 shows cross-sections of granules observed by transmission electron microscopy (TEM). Group A granules showed fairly large pores between the host particles, in a similar manner to the surface observed by SEM (cf. Fig. 2). Thus, the local density of group A granules was more or less homogeneous throughout the whole granule.

The internal structure of group B granules, on the other hand, was quite different from that of the surface. Host silica microspheres and aggregates of fine Aerosil particles, with wide size distribution of inter-particle voids, are clearly distinguishable. The density of the Aerosil aggregates was much higher at the surface, compared with that in the interior. A more densely packed structure was observed for those granules prepared from slurries of pH 3 and 11, as compared with those of pH 7. Hence, the difference in granule microstructure is attributed to the properties of the slurry.

3.2. Dehydration of the slurry

In a previous report [12], it was revealed that granule dispersion was dominated by electrostatic repulsion, or PVA adsorption, at pH higher or lower than 7, respectively. Differences in the state of dispersion were related to the rate of dehydration during drying and, hence, to the properties of spray-dried granules. As

shown in Fig. 4, isothermal dehydration profiles can be divided into two groups, i.e. slower dehydration of group B slurries at pH 3 and 11 compared to the others.

The smoother surface and denser near-surface region of group B granules prepared from pH 3 and 11 slurries are attributed to slower dehydration of these slurries. Due to better dispersion of added micro-particles, the aperture of water molecule effusion was smaller. For these slurries, the early steps of dehydration took place by out-flow of free water, containing well-dispersed Aerosil particles. They remained at the outermost region of the granule and restricted later vaporization of the remaining water. This was not the case for the group B slurry with pH 7, due to aggregation and to the related broader water pathway, being similar to group A slurries.

3.3. Pore size distribution

The above-mentioned difference tallies well with the results of porosimetry shown in Fig. 5. The pore size distribution of group A granules always showed its frequency maxima around 300 nm, while those from group B were much broader, without having sharp maxima. Closer observation of the group B granule, obtained from the pH 7 slurry, revealed the existence of pores at regions above 100 nm, close to those maxima for group A granules.

3.4. Pyrolysis of PVA in granules

The decomposition temperature of PVA was determined from the differential scanning calorimetry (DSC) peak temperature. As shown in Fig. 6, the decomposition temperature of PVA adhered to silica in a granule, was always significantly higher than that of PVA without silica, i.e. 287 °C. The shift of the PVA decomposition temperature was particularly large for those prepared at low pH, thus indicating the qualitative difference in the adhesion state of PVA with varying slurry pH. In other words, better adsorption of PVA in the slurry was maintained as a firmer adhesion

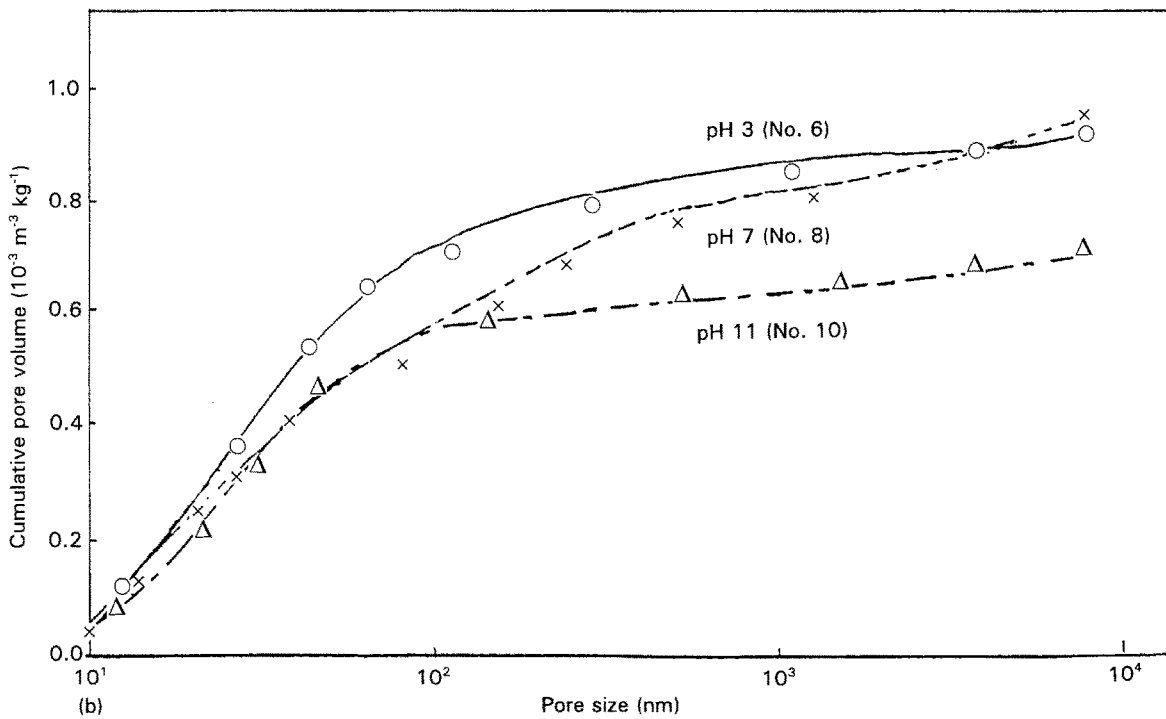
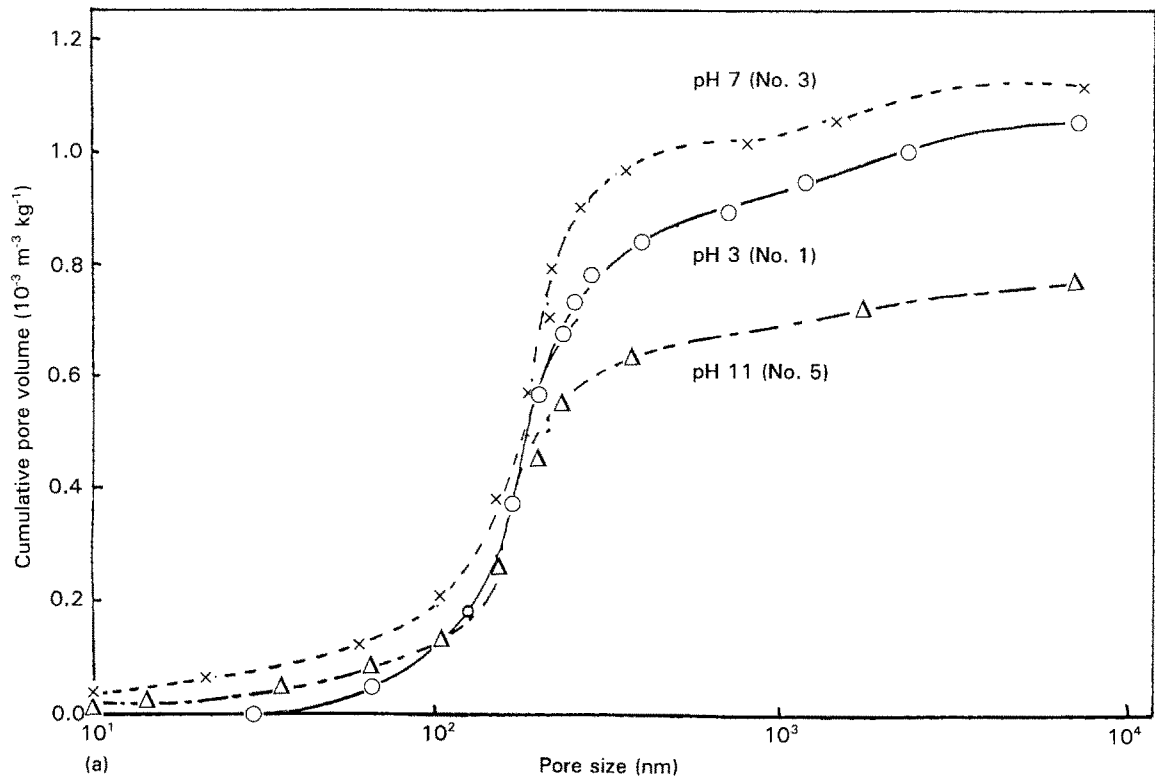


Figure 5 Representative pore size distribution. (a) A group and (b) B group.

after drying. This is quite reasonable, since adhesion of PVA to silica in a granule is still dominated by hydrogen bonding, with the aid of a small amount of water persistently existing on the silica surface. Adhesion of PVA in a dry granule is assumed to be achieved by such kinds of hydrogen bonds, together with conventional van der Waals bonds, keeping the intermolecular distance of PVA below 0.5 nm [13].

3.5. Structure–strength relationship

The compressive strength of the granule increased almost linearly with the apparent density, the latter

being estimated from the total pore volume. The inclination of the correlation was larger for group B granules. The higher compressive strength for group B granules, compared at the same pH, is attributed to stuffing of aerosil in the pores between host particles. Number 5 and 10 granules, prepared from slurries of $\text{pH} \geq 7$, showed highest strength and apparent density, while number 3 and 8 granules, from the neutral slurries, the lowest. The high strength and density of granules prepared at higher pH are attributed to better dispersion, due to electrostatic repulsion. In contrast, the high strength of granules prepared from low pH slurries is to be explained by firmer attach-

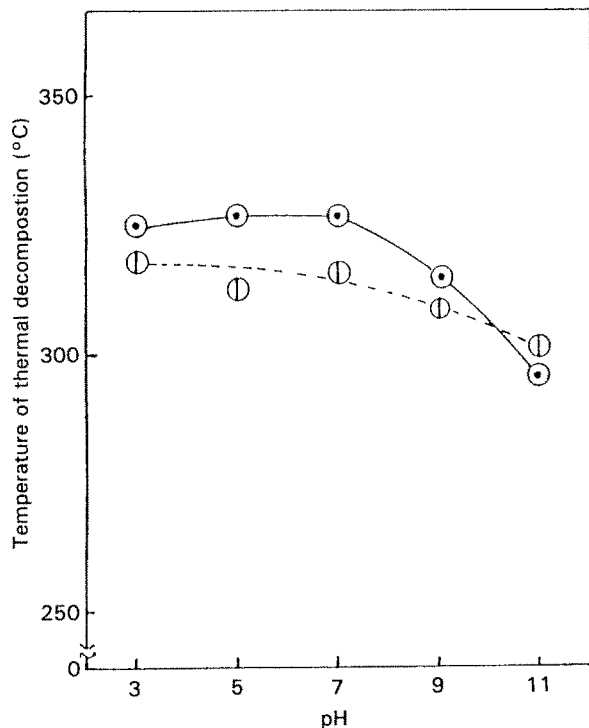


Figure 6 Relationship between decomposition temperature of PVA and pH of slurry from which granule was spray dried, using DSC.

ment of PVA onto the silica surface, resulting in higher efficiency of PVA as a binder.

4. Conclusions

The microstructure of silica-PVA granules was controlled by slurry pH, as a starting material. Granules prepared from slurries with $\text{pH} \geq 7$, with a higher absolute value of zeta potential, showed the highest apparent density. Granules prepared from pH 3 slurries, near the isoelectric point, were also dense due to better adsorption of PVA in the slurry, and firmer adhesion after drying. It was also indicated that radial distribution of the local density was also controllable, by adding microspheres and choosing the appropriate pH value.

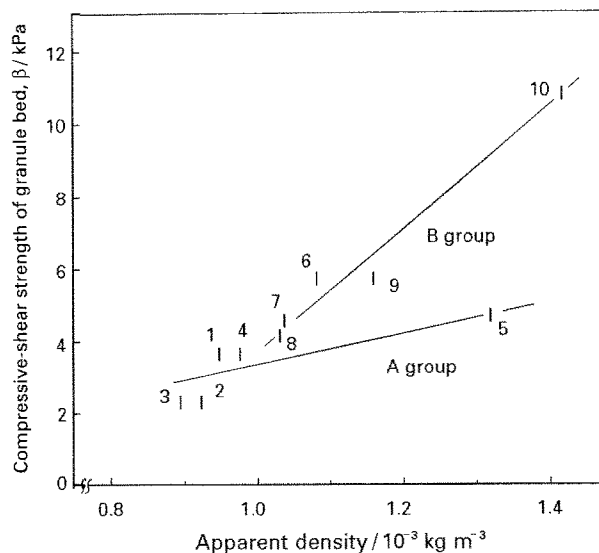


Figure 7 Relationship between compressive-shear strength of granule bed and apparent density.

References

1. H. YOKOYAMA, *Hyomen Kagaku* **13** (2) (1992) 49.
2. T. ISHIMORI and M. SENNA, *J. Soc. Powder Technol. Jpn.*, **30** (1993) 470.
3. S. TAKADA, *Funtai to Kougyou* **23** (1991) 43.
4. B. D. MOSSER, J. S. REES and J. R. VARNER, *Ceram. Bull.* **71** (1992) 105.
5. J. Y. KIM, M. INOUE, Z. KATO, N. UCHIDA, K. SAITO and K. UEMATU, *J. Mater. Sci.* **26** (1991) 2215.
6. K. FURUSAWA, *Hyomen* **15** (1977) 496.
7. A. TAKAHASHI, *Koubunshi* **32** (1983) 185.
8. R. K. ILER, *J. Colloid Interface Sci.* **51** (1975) 388.
9. T. F. TADROS, *ibid.* **64** (1978) 36.
10. T. ISHIMORI and M. SENNA, *Adv. Powder Technol.*, **4** (1993) 217.
11. D. G. THOMAS, *J. Colloid Sci.* **20** (1965) 267.
12. T. ISHIMORI and M. SENNA, *J. Soc. Rheol. Jpn* **22** (1994) 45.
13. A. D. McLAREN, *Mod. Plastics* **31** (1954) 114.

Received 24 May
and accepted 24 November 1993